Upregulation of (C-X-C motif) Ligand 13 (CXCL13) Attenuates Morphine Analgesia in Rats with Cancer-Induced Bone Pain

Authors' Contribution:
Study Design A
Data Collection B
Statistical Analysis C
Data Interpretation D
Manuscript Preparation E
Literature Search F
Funds Collection G

ABCDEF 1 **Shi-Feng Wang***
ABCDEF 2 **Cheng-Gong Dong***
EF 3 **Xue Yang**
DE 4 **Jian-Jun Yin**

1 Department of Pathology, South Medical District of Linyi People's Hospital, Linyi, Shandong, P.R. China
2 Department of Pathology, Yantaishan Hospital, Yantai, Shandong, P.R. China
3 Pediatric Rescue Room, Linyi People's Hospital, Linyi, Shandong, P.R. China
4 Health Management Center, Qingdao Hiser Medical Group, Qingdao, Shandong, P.R. China

Corresponding Author:
Source of support:

* Shi-Feng Wang and Cheng-Gong Dong both contributed equally to this research
Jian-Jun Yin, e-mail: yinjianjun_yjj@163.com
Departmental sources

Background: The aim of this study was to investigate the role of chemokine (C-X-C motif) ligand 13 (CXCL13) in morphine tolerance in rats with cancer-induced bone pain (CIBP).

Material/Methods: We established a rat CIBP model and a rat CIBP-morphine tolerance (BM) model. BM rats were intrathecally administered rmCXCL13, neutralizing anti-CXCL13, and normal saline, while the control group rats underwent a sham operation and were injected with normal saline. The morphine analgesia was assessed by measuring mechanical withdrawal threshold (MWT) and mechanical withdrawal duration (MWD) at various time points. The co-expressions of CXCL13 and NeuN were measured by immunofluorescence double-staining. CXCL13 protein and mRNA expressions were detected by Western blot and quantitative real-time polymerase chain reaction (RT-qPCR), respectively.

Results: Compared to the sham-operation (S) group, the BM group showed obviously decreased MWT and increased MWD on Day 9 after CIBP, but obviously increased MWT and decreased MWD on Day 3 after morphine administration; subsequently, the MWT was decreased and MWD was increased (all $P<0.05$). In comparison with the S+saline group, increased MWT and decreased MWD were observed in BM rats on Day 3 after anti-CXCL13 administration, and obviously decreased MWT and increased MWD were found in BM rats on Day 3 after rmCXCL13 administration (all $P<0.05$).

Conclusions: Up-regulated CXCL13 has a negative role in morphine analgesia in relief of CIBP, which may provide a new target for the management of CIBP.

MeSH Keywords: **Chemokine CXCL13 • Models, Animal • Rats**

Full-text PDF: **http://www.medscimonit.com/abstract/index/idArt/897702**

📄 4247   🗂 2   📊 6   📖 46

Background

Pain is the most common symptom in cancer patients. About 75–90% of patients with metastatic or advanced-stage cancer will suffer metastatic cancer-induced bone pain (CIBP), and the severity of CIBP is closely correlated with the extent of bone destruction [1–3]. CIBP is commonly induced by primary bone cancer or secondary bone metastasis from other malignancies, such as breast, prostate, and lung cancer, which may produce excruciating bone pain [4–6]. Generally, the primary treatment of CIBP is utilization of opioids and other adjuvants, such as morphine, nonsteroidal anti-inflammatory drugs, and cannabinoids [7]. Morphine relieves chronic and acute pain by binding the μ opioid receptor (MOR) on the sensory neurons in central and peripheral nervous systems, but adequate analgesia may not be achieved due to drug tolerance [8]. Tolerance to analgesia caused by repeated usage of morphine, the attenuation of analgesic efficacy, and the shortened analgesic duration may limit the long-term therapy of cancer patients [9]. Previous studies hypothesized several different mechanisms of morphine tolerance, such as content alterations in neurotransmitters, functional changes in receptors, and down-regulation of opioids receptors [10,11], but the exact underlying mechanisms of morphine tolerance are still unclear.

Recently, some chemokines, including C-X-C motif chemokine 10 (CXCL10), C-C motif ligand 2 (CCL2), CX3C chemokine receptor 1 (CX3CR1), and C-C motif ligand 5 (CCL5), have been studied in the spinal cord and may be involved in CIBP development [12–14]. CXCL13 is a kind of homeostatic chemokine that is constitutively secreted by stromal cells in the B cell areas of secondary lymphoid tissues [15]. Increased CXCL13 expression was found in systemic lupus erythematosus and correlated with disease activity, which might be a readily available surrogate marker to monitor the extent of aberrant B cell function [16]. CXCL13 may mediate B cell trafficking by interacting with C-X-C chemokine receptor type 5 (CXCR5) and is increased proportionately to disease activity in many antibody-mediated syndromes [17,18]. Commonly expressed in angio-immunoblastic T cell lymphoma, CXCL13 expression may be associated with the attraction of human metastatic neuroblastoma cells to bone marrow via mediating CXCR5 [19]. Chemokines and chemokine receptors have been reported to be involved in neuroinflammation at different anatomical locations and may contribute to chronic pain processing [20,21]. Inflammatory responses are frequently combined with the development of neuropathic pain, and chemokines have been reported to be crucial in integrating the occurrence of pain and inflammation [22–24]. NeuN is a neuronal nuclear antigen that is commonly used as a biomarker for neurons, and increased pJNK levels were co-expressed with NeuN (a neuron marker) in spinal cord and participated in CIBP in rats [25,26]. In addition, CXCL13 mRNA was colocalized with neuronal marker,

suggesting that CXCL13 is induced by neurons but not with markers of astrocytes or microglia, and neuronally produced CXCL13 activates astrocytes via CXCR5 to facilitate neuropathic pain [27]. The exact relationship between the expression of CXCL13 and NeuN in CIBP has not be clearly defined. In addition, chemokines and opioids are important regulators of immune, inflammatory, and neuronal responses in peripheral and central pain pathways [28]. However, it is not clear whether CXCL13 is involved in the mechanisms of tolerance to analgesic drugs, including morphine tolerance, in the management of cancer pain.

In the present study we examined the expression levels of CXCL13 protein and mRNA in spinal cord using a well-established rat model of CIBP, and investigated the role of CXCL13 in the occurrence and maintenance of CIBP. We also established a morphine tolerance model in CIBP rats to explore whether CXCL13 is involved in the development of morphine tolerance in CIBP rats, to provide a new target for cancer pain management.

Material and Methods

Animals and establishment of animal models

Experiments were performed on 100 specific pathogen-free (SPF) adult female Sprague–Dawley (SD) rats, weighing 180–200 g, from the Shanghai Experimental Animal Center (Shanghai, China; Certificate number: SCXK (Hu) 2013–002). Under a temperature-controlled condition (20–25°C), the rats were acclimatized in a clean-grade animal house with 40–70% humidity (aiming for 50%) with a 12/12 h light/dark cycle. All SD rats were acclimated to local vivarium conditions with appropriate airflow (indoor wind speed: 0.1–0.2 m/s) without draftiness. All studies were approved by the Institutional Animal Care and Academic Committee on the Ethics of Animal Experiments of Linyi People's Hospital and were performed in strict compliance with the Ethical Issues of the International Association for the Study of Pain. Efforts were exerted to reduce the number of animals used and to minimize their suffering.

Model of bone cancer pain

A rat model of bone cancer pain was established by the intrathecal injections of Walker 256 mammary gland carcinoma cells (10 μl, 4×10⁵ cells/mL, purchased from Shanghai Institutes for Biological Sciences) into the intramedullary space of the right proximal tibia in rats, as previously described [29]. Bone destruction was diagnosed by X-ray examination. Thirty rats were randomly separated into 3 groups: (1) healthy control group (C group, n=10) rats were subjected to no treatment; (2) sham-operation group (S group, n=10) rats underwent surgery,

but only exposed the right proximal tibia of rats; and (3) CIBP group (n=10) rats were used to establish the tibial cancer pain model. The mechanical withdrawal threshold (MWT) and mechanical withdrawal duration (MWD) of rats were measured on preoperative Day 1 (T_0) and on Days 3 (T_1), 6 (T_2), 9 (T_3), 12 (T_4), 15 (T_5), and 18 (T_6) after CIBP modeling. On Day 18, all rats in the 3 groups were decapitated. The co-expressions of CXCL13 and NeuN in neurons were measured by immunofluorescence double-staining and the expression levels of CXCL13 protein and mRNA were measured by Western blot and quantitative real-time polymerase chain reaction (RT-qPCR), respectively.

Model of bone cancer pain morphine tolerance (BM model)

After the rat model of bone cancer pain was successfully established for 9 days as previously described, the rats were intrathecally given morphine (20 µg/kg, diluted with the physiological saline up to 100 µl) twice daily (at 10: 00 am and 8: 00 pm) from Day 9 to Day 18, to establish the rat model of morphine tolerance. Thirty adult female SD rats were randomly divided into 3 groups: (1) sham-operation group (S group, n=10) rats were underwent surgery, but only exposed the right proximal tibia of rats; (2) morphine group (M group, n=10) the rats were intrathecally administered morphine 20 µg/kg (diluted with physiological saline up to 100 µl) twice daily from Day 9 to Day 18 after 10 µl of heat-inactivated Walker 256 cells were injected into tibial marrow cavity; and (3) bone cancer pain-morphine tolerance (BM group) rats were intrathecally administered 20 µg/kg morphine (diluted with the physiological saline up to 100 µl) twice daily from Day 9 to Day 18 after CIBP models were well-established by Walker256 carcinoma cells. The MWT and MWD of the rats were determined on pre-operative Day 1 (T_0), on Day 3 (T_1), 6 (T_2) and 9 (T_3) after CIBP modeling, and on Day 3 (T_4), 6 (T_5) and 9 (T_6) after intrathecally administering morphine. On Day 18, all rats in the 3 groups were decapitated. The expression levels of CXCL13 protein and mRNA were measured by Western blot and RT-qPCR, respectively.

Forty adult female SD rats were randomized into 4 groups. Rats in the S+saline group (n = 10) received sham operation of tibia and on Day 6 were intrathecally injected with 100 ng saline for 3 days. The remaining 30 rats had the BM model successfully established. Then, the rats were divided into 3 groups: (1) BM+rmCXCL13 group (n=10) rats were intrathecally injected with 30 ng rmCXCL13 for 3 days from Day 6 after the BM model was successfully established; (2) BM+anti-CXCL13 group (n=10) rats were intrathecally injected with 100 ng anti-CXCL13 neutralizing antibody for 3 days from Day 6 after the BM model was successfully established; and (3) BM+saline group (n=10) rats were intrathecally injected with 100 ng saline for 3 days from Day 6 after the BM model was successfully established. The MWT and MWD of the rats were used to

evaluate their behaviors on pre-operative Day 1 (T_0); on Days 3 (T_1), 6 (T_2), and 9 (T_3) after CIBP modeling; on Days 3 (T_4) and 6 (T_5) after intrathecally administering morphine; and on Day 3 (T_6) after intrathecally administering drugs (rmCXCL13, anti-CXCL13, and saline). Rats were decapitated after intrathecally administering drugs for 3 days. The expression levels of CXCL13 protein and mRNA were measured by Western blot and RT-qPCR, respectively.

Behavioral measurements

Determination of MWT

Rats were placed in plexiglas cages (10×10×15 cm) and acclimated for 15 min. All rats were tested for their withdrawal threshold of the plantar surface using Von Frey filaments stimulation. Von Frey filaments, with bending forces at 0.4, 0.6, 1.0, 2.0, 4.0, 6.0, 8.0, and 15.0 g, were used to stimulate the plantar surface in a progressively increasing manner for a continuous period of 3–5 s. Withdrawal of a hind paw upon the stimulus was defined as a positive response. In this study, filaments with 2.0 g bending force were used to stimulate the plantar surface. If the rat showed positive reaction, we reduced the bending force; but if the rat showed a negative reaction, we increased the bending force of Von Frey filaments. Each stimulus was repeated 5 times with 10-min intervals, and the mean was defined as MWT for this measurement. The data were calculated by the formula: $50\%MWT=10^{x+k\sigma}/10000$ (X defined as the last bending force; k defined as the coefficient; σ defined as the mean interval between the bending forces, σ=0.224).

Determination of MWD

Rats were also placed in plexiglas cages as previously described. A pin prick was used to stimulate the lateral part of the plantar surface of the paw in C group rats at an intensity sufficient to indent but not penetrate the skin. A stopwatch was used to record the duration of paw withdrawal, with an arbitrary minimal time of 0.5 s (for the brief normal response) and a maximal cut-off of l0 s.

Immunofluorescence double-staining

Rats were sacrificed after the measurement of withdrawal threshold. The rats were post-fixed in 4% paraformaldehyde through the left ventricle, the abdominal cavity was opened downward from the cartilago ensiformis, surrounding tissues and blood vessels were separated to expose the spine, the 4th spinal canal corresponding to the 12th rib was removed to obtain spinal cord from the L4–L6 segments, and the obtained spinal cord from the L4–L6 segments were immediately placed in liquid nitrogen for preservation and for further detection. The spinal cord from the L4–L6 segments were successively

soaked in 10% and 30% sucrose and dehydrated at 4°C until the tissues sank. Serial sections (30-μm-thick) of the spinal cord from the L4–L6 segments were made with a freezing microtome. The sections were washed in phosphate-buffered saline (PBS) and blocked with bovine serum albumin (BSA) for 30 min. After washing 3 times with PBS, the sections were incubated with the primary antibodies – goat anti-rat CXCL13 polyclonal antiserum (1:100; Santa Cruz, USA) and rabbit anti-rat NeuN (1:200; Chemicon, USA) – overnight at 4°C. Subsequently, sections were washed 3 times with PBS and incubated with secondary antibodies: Cy3-labeled anti-goat antibody (1:200; Jackson, USA) and FITC-labeled anti-rabbit IgG (1:200; Jackson, USA). After 2 h of incubation at room temperature, the sections were washed 3 times with PBS and blocked with 50% glycerin. Laser-scanning confocal microscopy (Eppendorf, Germany) was used to photograph the co-expression of CXCL13 and NeuN. The expression of CXCL13 and NeuN respectively appeared as red fluorescence and green fluorescence, and the co-expression of CXCL13 and NeuN appeared as yellow fluorescence.

Detection of the CXCL13 mRNA expression by RT-qPCR

The detection of CLCX13 mRNA expression was by RT-qPCR (Thermo, USA), and GAPDH was used as an endogenous reference for CLCX13. Total mRNA was extracted from the spinal cord from the L4-L6 segments using TRIzol reagent (Invitrogen) following the manufacturer's instructions. After the concentration of the purified mRNA was verified, we conducted reverse transcription. The reverse transcription reaction mix contained 2.5 μl buffer (supplemented with Mg), 0.5 μl dNTP, 0.4 μl Tap, 1 μl CXCL13 forward primers, 1 μl CXCL13 reverse primers, 2 μl template DNA, and 12.6 μl H_2O. The forward primers and reverse primers of CXCL13 were 5'-CTGCTCGGAATCTTAGTGT-3' and 5'-GGTAATGCGTCTGCTTCT-3', respectively. The forward primers and reverse primers of glyceraldehyde-3-phosphate dehydrogenase (GAPDH) were 5'-GGCACAGTCAAGGCTGAATG-3' and 5'-ATGGTGGTGAAGACGCCAGTA-3', respectively. The PCR reaction conditions were initial denaturation at 95°C for 30 s and 40 cycles of denaturation at 95°C for 8 s and annealing/extension at 60°C for 32 s. The cycle number at threshold (Ct value) was used to calculate the relative amount of CXCL13 mRNA molecules. The results are presented as fold-change, calculated using the $2^{-\Delta\Delta CT}$ method [30].

Western blot for CXCL13 protein expression

Western blot analysis was used to detect CXCL13 protein level. The spinal cord from the L4-L6 segments were lysed in protein extraction buffer and the protein concentration was determined by bicinchoninic acid (BCA) assay and denaturation at 95°C for 10 min. Total 50 μg protein (20μl) was separated by 5% sodium dodecyl sulfate-polyacrylamide gel electrophoresis

(SDS-PAGE) using constant 80 V voltage, and then the 12% separating gel were electrophoresed with constant 100 V voltage for 3 h and transferred to polyvinylidene difluoride filter membranes at room temperature for 2 h using a wet transfer system under a constant 295 mA current. After blocking with 5% non-fat dry milk at room temperature for 1 h in Tris-buffered saline containing 0.1% Tween-20 (TBST; washed 3 times), membranes were incubated with primary antibodies: goat anti-rat CXCL13 polyclonal antiserum (1:100; Santa Cruz, USA) and mouse anti-rat β-actin (1:2000; CST, USA) at 4°C overnight. Following primary antibody incubations, membranes were washed 3 times with TBST and incubated with secondary antibodies: rabbit anti-goat IgG (1:5000; Jackson, USA) and rabbit anti-rat IgG (1:5000; Jackson, USA) for 2 h at room temperature, and visualized by a standard chemical luminescence method. The Gel Documentation System was used to identify the integral optical density of the bands in the gels. The integral optical density of each band was calculated, and the relative expression of CXCL13 was the ratio of the integral optical density of CXCL13 and β-actin.

Statistical method

SPSS 21.0 statistical software (SPSS Inc., Chicago, IL) was used for statistical analysis. The measurement data are expressed by mean and standard deviation ($\bar{\chi}\pm s$). Normality test and variance homogeneity test were used in comparison between groups. One-way ANOVA analysis was used for multiple group comparisons. The LSD t test was used in comparison of multiple groups' averages. Differences of comparisons between different time points were made by repeated measures ANOVA. $P<0.05$ was considered statistically significant.

Results

CIBP model was successfully established

The rats in the S group and CIBP group were in basically normal state of drinking and eating, and the wounds of rats were well healed and rats were in good vitality state. The mental state of rats in the CIBP group became worse, with poor appetite and the body weight of rats only had a low increase from Day 9. Until Day 15, the body weight of rats in the CIBP group seems to be a downward trend; however, the rats in the S group were in good condition. Compared with the C group, the body weight of rats in the S group at each time point had no significant difference (all $P>0.05$). In comparison to the S group and C group, the body weight of rats in the CIBP group was significantly different at time points T_{3-6} (all $P<0.05$).

There were no obvious differences in MWT and MWD of rats at each time point of preoperative and postoperative periods

between the C group and S group (all *P*>0.05). The X-ray results showed no obvious bone destruction in the S group at each time point. Compared with the C group and S group, the MWT and MWD were significantly different in the CIBP group at time points T_{3-6} (all *P*<0.05) (Table 1). X-ray imaging indicated that rats in the CIBP group had obvious bone destruction from Day 9 (T_3) after CIBP modeling (Figure 1). The value of MWT at T_{3-6} in the CIBP group was obviously decreased, while the value of MWD at T_{3-6} in the CIBP group was obviously increased, as compared to the values of MWT and MWD at T_{0-2}, respectively. The value of MWT was continuously decreased and the value of MWD was continuously increased at T_{4-6} in the CIBP group (all *P*<0.05), suggesting that the CIBP model was successfully established.

The expression levels of CXCL13 protein and mRNA in rats with CIBP

Immunofluorescence double-staining results showed that CXCL13 was more highly expressed in the spinal cord neurons of the CIBP group as compared to the C group and S group, indicating that neuropathic pain may induce the up-regulation of CXCL13 expression level, and the activation of astrocytes was inhibited (Figure 2). No significant differences in the expression levels of CXCL13 protein and mRNA were observed between the C group and S group (both *P*>0.05). However, the expression levels of CXCL13 protein and mRNA in the CIBP group were obviously increased in comparison to the C group and S group (both *P*<0.05) (Figure 3).

BM model was successfully established

The rats in the 3 groups were in good health during the experiments, and the body weight of rats had a low increase, but no obvious difference in body weight was found between each time point (all *P*>0.05). Compared with the S group, the value of MWT in M group rats declined at time points T_5 and T_6, while the value of MWD increased (all *P*<0.05). In the BM group, the value of MWT of rats declined at the time points of T_{3-6} but the MWD increased compared with the S group (all *P*<0.05). Compared to the M group, the values of MWT in the BM group declined at the time points of T_3, T_5, and T_6, but the MWD increased (all *P*<0.05). There were no significant differences in MWT and MWD in the S group at each time point during the whole process (both *P*>0.05). In the BM group, the value of MWT declined significantly and the MWD increased obviously at the time point of T_3; but at the time point of T_4, MWT rose and MWD declined to the values at the time point of T_2. Moreover, at the time points of T_5 and T_6, the value of MWT was obviously reduced, and the value of MWD was obviously increased (all *P*<0.05). These results demonstrate that morphine has good analgesic effect on bone cancer pain (Figure 4).

Changes of CXCL13 protein and mRNA levels in BM rats

The expression levels of CXCL13 protein and mRNA after intrathecally administering morphine for 9 days were measured by Western blot and RT-qPCR, respectively (Figure 5). The expression levels of CXCL13 protein and mRNA in the M group were reduced as compared to the S group, but no significant differences were observed between the 2 groups (both *P*>0.05). However, the expression levels of CXCL13 protein and mRNA in the BM group were significantly higher than those in the S group and M group (all *P*<0.05).

Effects of CXCL13 on morphine tolerance in rats with bone cancer pain

No significant differences were observed on MWT and MWD of rats in the S+saline group at different time points, and at the time points of T_{3-5}, there were no significant differences in MWT and MWD among the BM+saline group, BM+rmCXCL13 group, and BM+anti-CXCL13 group (all *P*>0.05). However, the MWT and MWD at the time points of T_{3-5} in these 3 groups had significant differences as compared to the S+saline group (all *P*<0.05). On Day 3 after intrathecally administering anti-CXCL13, in the BM+anti-CXCL13 group the value of MWT was significantly increased, MWD was significantly decreased, and these differences were significantly different as compared to the S+saline group (all *P*<0.05). In addition, the value of MWT was significantly decreased and MWD was significantly increased in the BM+rmCXCL13 group on Day 3 after intrathecally administering rmCXCL13, and these differences were significantly different compared to the S+saline group (all *P*<0.05). In the BM+saline group and BM+rmCXCL13 group, the expression levels of CXCL13 protein and mRNA were significantly higher on Day 3 after intrathecally administering drugs as compared to the S+saline group (all *P*<0.05). Furthermore, the expression levels of CXCL13 protein and mRNA in the BM+rmCXCL13 group were significantly higher than those in the BM+saline group (*P*<0.05). We also found that the expression levels of CXCL13 protein and mRNA in the BM+anti-CXCL13 group were higher than that in the S+saline group, but with no significant differences (*P*>0.05) (Table 2, Figure 6).

Discussion

In this study, we further investigated the expression levels of CXCL13 protein and mRNA in the spinal cord of rats with CIBP and explored the role of CXCL13 in the development of morphine tolerance in rats with CIBP. The results showed that the expression levels of CXCL13 protein and mRNA in the spinal cord were obviously increased in rats with CIBP, suggesting that the increased CXCL13 expression levels contributed to the development of CIBP in rats. Further, we found that the

Table 1. The changes of body weight, MWT and MWD of rats at different time points (n=10, $\bar{\chi} \pm$ s).

| Time	Weight			MWT			MWD		
	C	S	CIBP	C	S	CIBP	C	S	CIBP
T_0	186.85±2.94	187.20±3.06	187.05±2.99	14.12±1.83	14.20±1.95	14.18±2.06	0.75±0.26	0.70±0.26	0.70±0.26
T_1	199.35±2.52	196.20±4.63	195.40±4.38	13.85±1.77	14.03±1.68	13.61±1.89	0.80±0.26	0.80±0.35	0.80±0.35
T_2	209.05±3.24	206.03±4.42	204.05±6.27	14.07±1.82	13.88±1.75	12.09±2.11	0.75±0.26	0.75±0.35	0.95±0.28
T_3	221.25±4.93	217.70±4.92	207.20±5.97*#	14.16±1.78	13.91±1.80	9.54±1.56*#	0.80±0.26	0.80±0.35	3.15±1.06*#
T_4	231.50±4.22	231.95±4.13	212.80±5.62*#	13.94±1.69	13.56±1.63	8.42±1.19*#	0.80±0.26	0.80±0.34	5.15±1.20*#
T_5	239.50±5.12	237.75±5.15	217.55±5.90*#	14.08±1.84	13.81±1.79	7.87±0.98*#	0.75±0.26	0.80±0.26	5.40±1.13*#
T_6	245.40±5.57	243.10±6.10	215.65±6.25*#	14.13±1.75	13.52±1.74	7.03±1.04*#	0.80±0.26	0.80±0.35	5.60±1.02*#

C group – healthy control group; S group – sham-operation group; CIBP group – cancer-induced bone pain group; MWT – mechanical withdrawal threshold; MWD – mechanical withdrawal duration; T_0 – pre-operative Day 1; T_{1-6} – Day 3, 6, 9, 12 and 18 post CIBP modeling, respectively. * Compared with C group, $P<0.05$; # Compared with S group, $P<0.05$.
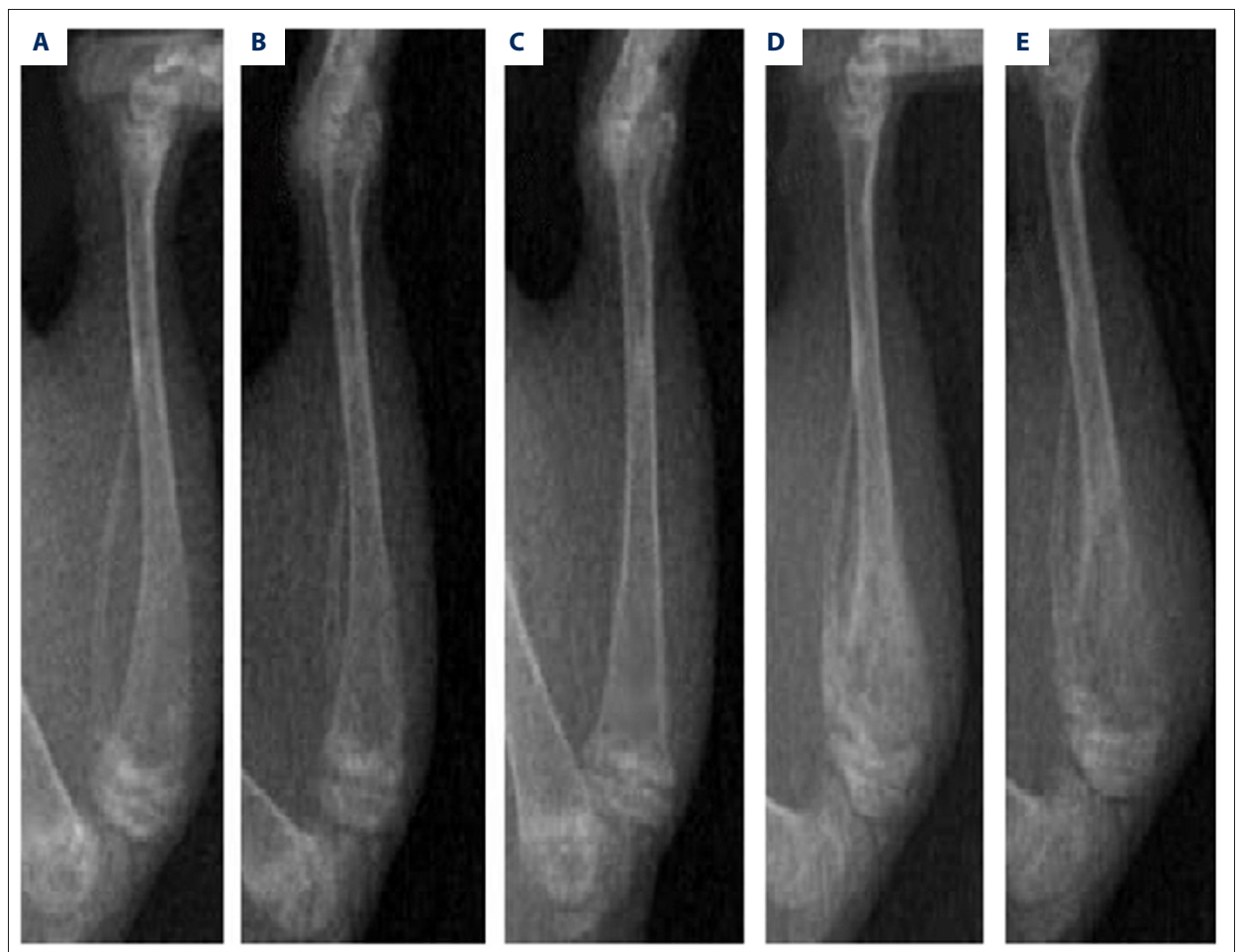

Figure 1. X-ray images of the right proximal tibia of rats. C group, healthy control group; S group, sham-operation group; CIBP group, cancer-induced bone pain group. (A) X-ray image of the healthy control rats (C group); (B) X-ray image of sham-operation rats (S group); (C) X-ray image of the rats on Day 6 post CIBP modeling; (D) X-ray image of the rats on Day 9 post CIBP modeling; (E) X-ray image of the rats on Day 12 post CIBP modeling.
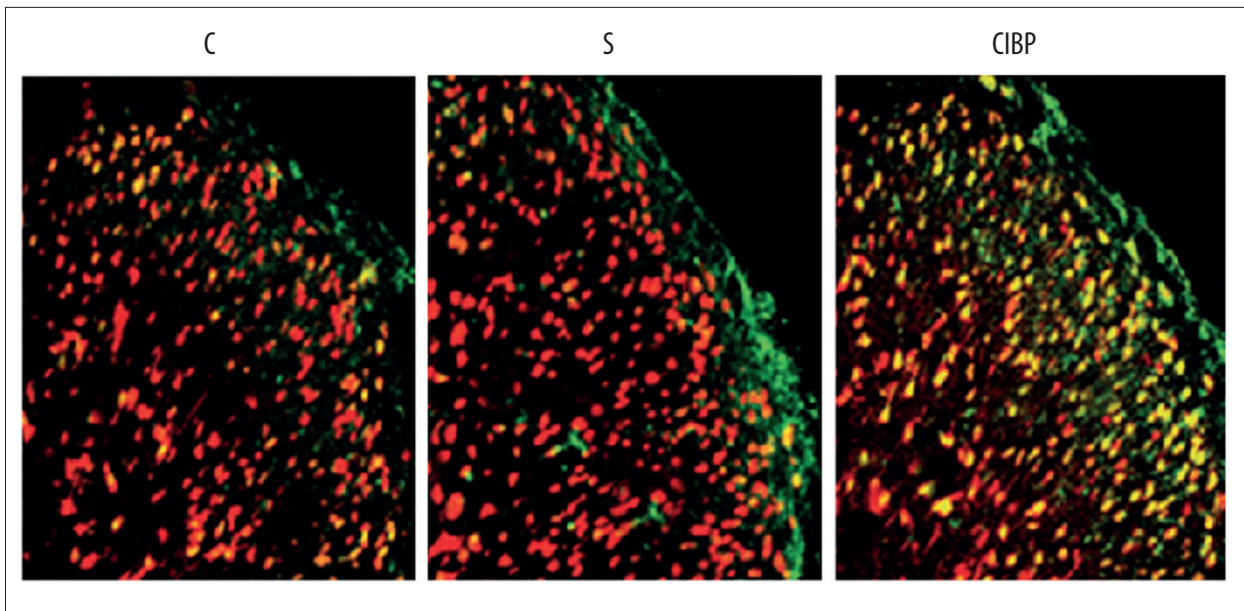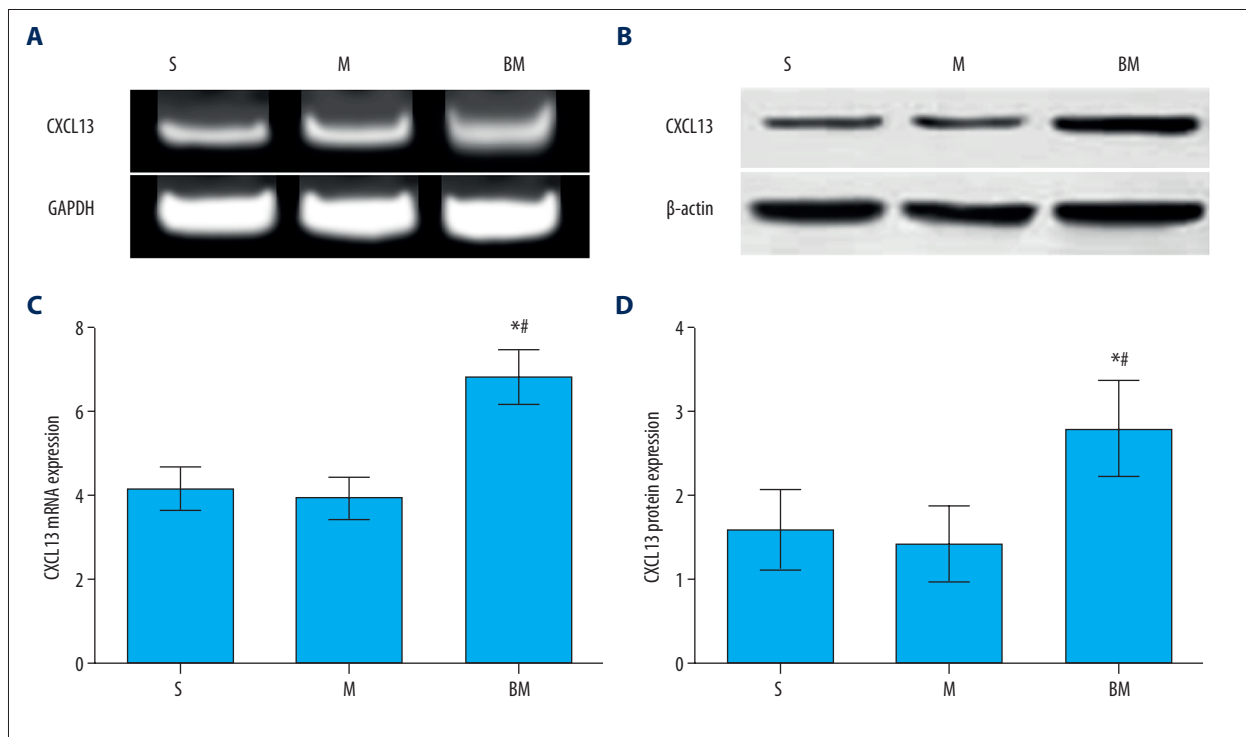
Figure 2. The expression levels of CXCL13 protein and mRNA detected by immunofluorescence double-staining (200×). C, healthy control group; S, sham-operation group; CIBP, cancer-induced bone pain group; Red fluorescence: the expression of CXCL13; Green fluorescence: the expression of NeuN; Yellow fluorescence: the co-expression of CXCL13 and NeuN.
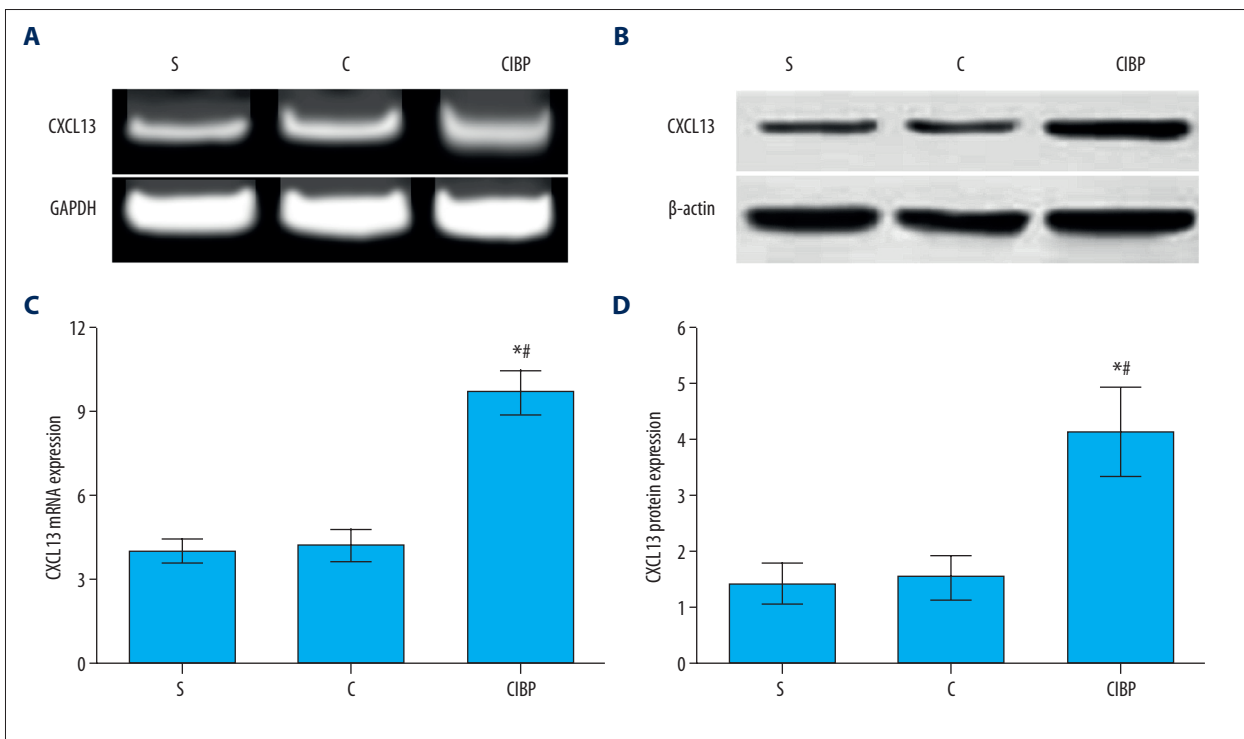
Figure 3. The expression levels of CXCL13 protein and mRNA on postoperatively Day 18 were detected by Western blot and RT-qPCR, respectively. C group, healthy control group; S group, sham-operation group; CIBP group, cancer-induced bone pain group. (**A**) The expression of CXCL13 mRNA was examined by RT-qPCR. (**B**) The expression of CXCL13 protein was examined by Western blot. (**C**) CXCL13 mRNA expression in CIBP group was significantly higher than that in the C group and S group; (**D**) CXCL13 protein expression in CIBP group was significantly higher than that in the C group and S group. * Compared with C group, $P<0.05$; # compared with S group, $P<0.05$.
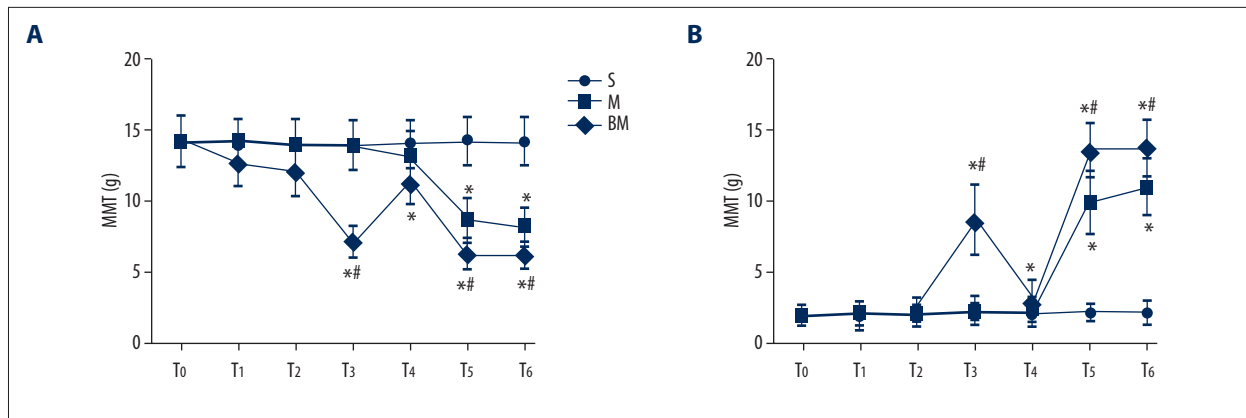
Figure 4. Changes in MWT and MWD of rats at each time point. S group, sham-operation group; M group, morphine group; BM group, bone cancer pain morphine tolerance group; MWT, mechanical withdrawal threshold; MWD, mechanical withdrawal duration; T_0: pre-operative Day 1; T_{1-3}: Day 3, 6, and 9 post CIBP modeling; T_{4-6}: Day 3, 6 and 9 after intrathecally administering morphine. (**A**) The changes of MWT of rats at each time point in these 3 groups; (**B**) The changes of MWD of rats at each time point in these 3 groups. * Compared with S group, $P<0.05$; # compared with M group, $P<0.05$.

Figure 5. The expression levels of CXCL13 protein and mRNA after 9 days of intrathecally administering morphine were measured by Western blot and RT-qPCR, respectively. S group, sham-operation group; M group, morphine group; BM group, bone cancer pain morphine tolerance group. (**A**) The expression of CXCL13 mRNA was examined by RT-qPCR. (**B**) The expression of CXCL13 protein was examined by Western blot. (**C**) CXCL13 mRNA expression in the BM group was significantly higher than that in the S group and M group; (**D**) CXCL13 protein expression in the BM group was significantly higher than that in the S group and M group. * Compared with S group, $P<0.05$; # Compared with M group, $P<0.05$.

CXCL13 protein reduced the value of MWT and increased the value of MWD, and the blocking function of CXCL13 by neutralizing anti-CXCL13 antibody may enhance morphine analgesia. These results indicate that CXCL13 may be involved in the occurrence of morphine tolerance in rats with CIBP, and the increased CXCL13 may play a negative role in morphine analgesia in relief of CIBP.

Table 2. The changes of MWT and MWD of rats at different time points ($n=10$, $\bar{x}\pm s$).

Time	MWT				MWD			
	S+ saline	BM+ saline	BM+ rmCXCL13	BM+ anti-CXCL13	S+ saline	BM+ saline	BM+ rmCXCL13	BM+ anti-CXCL13
T_0	14.15±1.70	14.09±1.72	14.18±1.63	14.16±1.55	0.80±0.26	0.85±0.24	0.75±0.26	0.85±0.24
T_1	14.08±1.66	12.62±1.61	12.46±1.53	12.67±1.58	0.85±0.34	0.80±0.35	0.85±0.34	0.80±0.35
T_2	14.10±1.69	11.78±1.65	11.83±1.54	11.85±1.49	0.80±0.26	0.95±0.37	0.95±0.28	0.90±0.39
T_3	13.97±1.54	7.22±1.09*	6.96±1.07*	7.14±1.16*	0.75±0.26	3.55±1.01*	3.65±1.25*	3.55±1.14*
T_4	14.06±1.67	11.45±1.47*	11.28±1.35*	11.49±1.40*	0.75±0.26	1.30±0.35*	1.25±0.35*	1.20±0.26*
T_5	14.18±1.59	6.48±0.98*	6.55±1.06*	6.64±1.12*	0.80±0.26	5.05±0.96*	5.10±0.97*	4.95±1.01*
T_6	14.05±1.58	6.31±1.02*	3.18±0.53*#	11.56±1.43*#&	0.75±0.26	5.40±1.02*	7.75±1.77*#	1.15±0.24*#&

MWT – mechanical withdrawal threshold; MWD – mechanical withdrawal duration; S+saline group – rats were underwent sham operation and injected with saline; BM+saline group – rats with bone cancer pain-morphine tolerance and injected with saline; BM+rmCXCL13 group – BM rats injected with rmCXCL13; BM+anti-CXCL13 group – BM rats injected with anti-CXCL13.
T_0 – pre-operative Day 1; T_{1-3} – Day 3, 6 and 9 post CIBP modeling; T_{4-5} – Day 3 and 6 after intrathecally administering morphine; T_6 – Day 3 intrathecally administering drugs. * Compared with S+saline group, $P<0.05$; # Compared with BM+saline group, $P<0.05$; & Compared with BM+rmCXCL13 group, $P<0.05$.
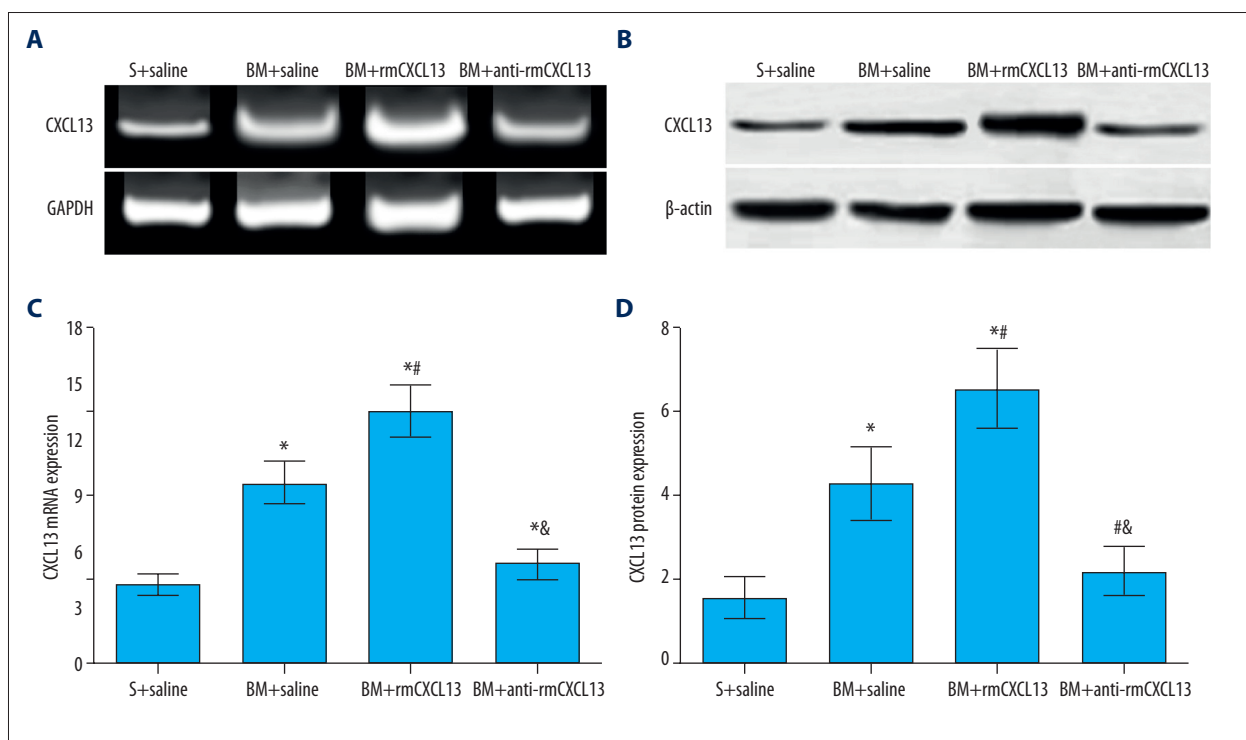
Figure 6. The expression levels of CXCL13 protein and mRNA after 3 days of intrathecally administering drugs (saline, anti-CXCL13, or rmCXCL13) were measured by Western blot and RT-qPCR, respectively. S+saline group: rats underwent sham operation and were injected with saline; BM+saline group: rats with bone cancer pain morphine tolerance and injected with saline; BM+rmCXCL13 group: BM rats injected with rmCXCL13; BM+anti-CXCL13 group: BM rats injected with anti-CXCL13 neutralizing antibody. (**A**) The expression of CXCL13 mRNA after intrathecally administering drugs was examined by RT-qPCR. (**B**) The expression of CXCL13 protein after 3 days of intrathecally administering drugs was examined by Western blot. (**C**) The comparisons of CXCL13 mRNA expression among the 4 groups; (**D**) The comparisons of CXCL13 protein expression among the 4 groups. * Compared with S+saline group, $P<0.05$; # Compared with BM+saline group, $P<0.05$; & Compared with BM+rmCXCL13 group, $P<0.05$.

It was well known that chemokines may induce the directional migration of cells, particularly of leukocytes during inflammation, and the prolonged inflammation may facilitate carcinogenesis by providing a microenvironment for the growth of tumor cells [31]. Acting as an important chemokine, CXCL13 is pivotal in establishing adaptive immune response, which may attract B cells, and facilitates the production of antibodies and local inflammation [32,33]. Additionally, CXCL13 expression is up-regulated by TNF-α and by T cell receptor stimulation [34,35]. CXCL13 could also serve as a marker reflecting the local activity of inflammation of diseases [35,36]. It has been reported that the CXCR5-CXCL13 axis is critical to the generation of immunological memory, as the interaction between T follicular helper and B cells plays a key role in the formation of plasma cells and autoantibody production [34,37]. Moreover, Singh et al. found that the CXCR5-CXCL13 axis may be involved in the cell migration, invasion, and adhesion of prostate cancer [38]. On the other hand, the alterations of chemokines expression combined with chemokines receptors may be associated with the generation and maintenance of neuropathic pain or chronic pain, and the up-regulation of chemokines in the spinal cord has been reported to be essential to the development of cancer pain [39,40]. CXCL1 has been reported to be up-regulated in astrocytes after spinal nerve ligation and contribute to the maintenance of neuropathic pain, and the increased CXCL1 expression may be involved in CIBP development [41]. A previous study has demonstrated that the increased expression levels of CX3CR1 in the spinal cord may play a key role in facilitating pain processing in rats with bone cancer pain [13]. In our study, both Western blot and RT-qPCR results showed that CXCL13 was highly expressed in the spinal cord after the CIBP model was well-established; indicating that the neuropathic pain may induce the up-regulation of CXCL13 expression level and inhibit astrocyte activation, and CXCL13 may be closely associated with the development of CIBP.

In the present study we also found that the CXCL13 protein and mRNA expression levels were significantly higher in BM rats, and the value of MWT increased significantly and the MWD obviously decreased in BM rats after injection with anti-CXCL13

neutralizing antibody. These results suggest that activation of the CXCL13 pathway may be essential to the occurrence and maintenance of CIBP, and blocking the function of CXCL13 by neutralizing antibodies could inhibit the development of morphine tolerance and enhance morphine analgesia. Morphine relieves pain by binding the MOR on the sensory neurons in the central and peripheral nervous systems, but the tolerance of morphine may weaken the analgesia effects [4,42]. The decrease of MOR in specific subpopulations of primary afferent neurons in the spinal cord may affect the analgesia effects [43]. It has been reported that morphine may induce the release of nitric oxide synthase of the primary sensory neuron, which may lead to hyperpolarization of neurons, which can produce the analgesia effect [44], while the chemokines may inhibit the hyperpolarization of neurons in the periaqueductal gray (PAG) areas that are induced by morphine [45]. Further, the chemokine interactions with the opioid neuropeptide system may inhibit opioid analgesics in the treatment of inflammatory pain [46]. In this regard, we suspect that CXCL13 suppresses the morphine-induced hyperpolarization of sensory neurons in the spinal cord by inducing the interaction between its receptor and MOR, which may weaken the morphine analgesia. Therefore, the inhibition of CXCL13 expression may prevent the development of morphine tolerance and enhance morphine analgesia, which is in line with our study results.

Conclusions

We found increased expression levels of CXCL13 protein and mRNA in rats with CIBP, indicating that the chemokine CXCL13 plays a key role in the occurrence of morphine tolerance in rats with CIBP, and the up-regulated expression of CXCL13 may play a negative role in morphine analgesia in relief of CIBP. Blocking CXCL13 function by neutralizing anti-CXCL13 antibody may be key to enhanced morphine analgesia.

Disclosure statement

We declare no conflict of interest.

References:

1. Kumar SP: Cancer Pain: A critical review of mechanism-based classification and physical therapy management in palliative care. Indian J Palliat Care, 2011; 17: 116–26

2. Kane CM, Hoskin P, Bennett MI: Cancer induced bone pain. BMJ, 2015; 350: h315

3. Colvin L, Fallon M: Challenges in cancer pain management – bone pain. Eur J Cancer, 2008; 44: 1083–90

4. Jimenez-Andrade JM, Mantyh WG, Bloom AP et al: Bone cancer pain. Ann NY Acad Sci, 2010; 1198: 173–81

5. Bloom AP, Jimenez-Andrade JM, Taylor RN et al: Breast cancer-induced bone remodeling, skeletal pain, and sprouting of sensory nerve fibers. J Pain, 2011; 12: 698–711

6. Slosky LM, Largent-Milnes TM, Vanderah TW: Use of animal models in understanding cancer-induced bone pain. Cancer Growth Metastasis, 2015; 8: 47–62

7. Middlemiss T, Laird BJ, Fallon MT: Mechanisms of cancer-induced bone pain. Clin Oncol (R Coll Radiol), 2011; 23: 387–92

8. Caraceni A, Hanks G, Kaasa S et al: Use of opioid analgesics in the treatment of cancer pain: evidence-based recommendations from the EAPC. Lancet Oncol, 2012; 13: e58–68

9. Iwai S, Kiguchi N, Kobayashi Y et al: Inhibition of morphine tolerance is mediated by painful stimuli via central mechanisms. Drug Discov Ther, 2012; 6: 31–37

10. Ueda H, Ueda M: Mechanisms underlying morphine analgesic tolerance and dependence. Front Biosci (Landmark Ed), 2009; 14: 5260–72

11. Xu JT, Zhao JY, Zhao X et al: Opioid receptor-triggered spinal mTORC1 activation contributes to morphine tolerance and hyperalgesia. J Clin Invest, 2014; 124: 592–603

12. Bu H, Shu B, Gao F et al: Spinal IFN-gamma-induced protein-10 (CXCL10) mediates metastatic breast cancer-induced bone pain by activation of microglia in rat models. Breast Cancer Res Treat, 2014; 143: 255–63

13. Hu JH, Yang JP, Liu L et al: Involvement of CX3CR1 in bone cancer pain through the activation of microglia p38 MAPK pathway in the spinal cord. Brain Res, 2012; 1465: 1–9

14. Hu JH, Zheng XY, Yang JP, Wang LN, Ji FH: Involvement of spinal monocyte chemoattractant protein-1 (MCP-1) in cancer-induced bone pain in rats. Neurosci Lett, 2012; 517: 60–63

15. Ansel KM, Harris RB, Cyster JG: CXCL13 is required for B1 cell homing, natural antibody production, and body cavity immunity. Immunity, 2002; 16: 67–76

16. Schiffer L, Kumpers P, Davalos-Misslitz AM et al: B-cell-attracting chemokine CXCL13 as a marker of disease activity and renal involvement in systemic lupus erythematosus (SLE). Nephrol Dial Transplant, 2009; 24: 3708–12

17. Rupprecht TA, Plate A, Adam M et al: The chemokine CXCL13 is a key regulator of B cell recruitment to the cerebrospinal fluid in acute Lyme neuroborreliosis. J Neuroinflammation, 2009; 6: 42

18. Lee HT, Shiao YM, Wu TH et al: Serum BLC/CXCL13 concentrations and renal expression of CXCL13/CXCR5 in patients with systemic lupus erythematosus and lupus nephritis. J Rheumatol, 2010; 37: 45–52

19. Vandercappellen J, Van Damme J, Struyf S: The role of CXC chemokines and their receptors in cancer. Cancer Lett, 2008; 267: 226–44

20. Abbadie C, Bhangoo S, De Koninck Y et al: Chemokines and pain mechanisms. Brain Res Rev, 2009; 60: 125–34

21. Gao YJ, Ji RR: Chemokines, neuronal-glial interactions, and central processing of neuropathic pain. Pharmacol Ther, 2010; 126: 56–68

22. White FA, Bhangoo SK, Miller RJ: Chemokines: integrators of pain and inflammation. Nat Rev Drug Discov, 2005; 4: 834–44

23. Rittner HL, Brack A, Stein C: Pain and the immune system. Br J Anaesth, 2008; 101: 40–44

24. Kiguchi N, Kobayashi Y, Kishioka S: Chemokines and cytokines in neuroinflammation leading to neuropathic pain. Curr Opin Pharmacol, 2012; 12: 55–61

25. Mullen RJ, Buck CR, Smith AM: NeuN, a neuronal specific nuclear protein in vertebrates. Development, 1992; 116: 201–11

26. Wang XW, Hu S, Mao-Ying QL et al: Activation of c-jun N-terminal kinase in spinal cord contributes to breast cancer induced bone pain in rats. Mol Brain, 2012; 5: 21

27. Jiang BC, Cao DL, Zhang X et al: CXCL13 drives spinal astrocyte activation and neuropathic pain via CXCR5. J Clin Invest, 2016; 126: 745–61

28. Melik Parsadaniantz S, Rivat C, Rostene W et al: Opioid and chemokine receptor crosstalk: a Promising target for pain therapy? Nat Rev Neurosci, 2015; 16: 69–78

29. Li XQ, Sun YM, Huang ZX, et al: A rat model of tibia cancer pain produced by Walker 256 mammary gland carcinoma cells. Chinese Journal of Cancer Biotherapy, 2008; 15

30. Livak KJ, Schmittgen TD: Analysis of relative gene expression data using real-time quantitative PCR and the 2(-Delta Delta C(T)) Method. Methods, 2001; 25: 402–8

31. Balkwill FR: The chemokine system and cancer. J Pathol, 2012; 226: 148–57

32. van de Pavert SA, Olivier BJ, Goverse G et al: Chemokine CXCL13 is essential for lymph node initiation and is induced by retinoic acid and neuronal stimulation. Nat Immunol, 2009; 10: 1193–99

33. Ammirante M, Shalapour S, Kang Y et al: Tissue injury and hypoxia promote malignant progression of prostate cancer by inducing CXCL13 expression in tumor myofibroblasts. Proc Natl Acad Sci USA, 2014; 111: 14776–81

34. Manzo A, Vitolo B, Humby F et al: Mature antigen-experienced T helper cells synthesize and secrete the B cell chemoattractant CXCL13 in the inflammatory environment of the rheumatoid joint. Arthritis Rheum, 2008; 58: 3377–87

35. Kobayashi S, Murata K, Shibuya H et al: A distinct human CD4+ T cell subset that secretes CXCL13 in rheumatoid synovium. Arthritis Rheum, 2013; 65: 3063–72

36. Rosengren S, Wei N, Kalunian KC et al: CXCL13: a novel biomarker of B-cell return following rituximab treatment and synovitis in patients with rheumatoid arthritis. Rheumatology (Oxford), 2011; 50: 603–10

37. Wengner AM, Hopken UE, Petrow PK et al: CXCR5- and CCR7-dependent lymphoid neogenesis in a murine model of chronic antigen-induced arthritis. Arthritis Rheum, 2007; 56: 3271–83

38. Singh S, Singh R, Sharma PK et al: Serum CXCL13 positively correlates with prostatic disease, prostate-specific antigen and mediates prostate cancer cell invasion, integrin clustering and cell adhesion. Cancer Lett, 2009; 283: 29–35

39. Guo G, Gao F: CXCR3: latest evidence for the involvement of chemokine signaling in bone cancer pain. Exp Neurol, 2015; 265: 176–79

40. Zhou YQ, Gao HY, Guan XH et al: Chemokines and their receptors: potential therapeutic targets for bone cancer pain. Curr Pharm Des, 2015; 21: 5029–33

41. Xu J, Zhu MD, Zhang X et al: NFkappaB-mediated CXCL1 production in spinal cord astrocytes contributes to the maintenance of bone cancer pain in mice. J Neuroinflammation, 2014; 11: 38

42. Nakamura A, Hasegawa M, Minami K et al: Differential activation of the mu-opioid receptor by oxycodone and morphine in pain-related brain regions in a bone cancer pain model. Br J Pharmacol, 2013; 168: 375–88

43. Liu S, Liu WT, Liu YP et al: Blocking EphB1 receptor forward signaling in spinal cord relieves bone cancer pain and rescues analgesic effect of morphine treatment in rodents. Cancer Res, 2011; 71: 4392–402

44. Cunha TM, Roman-Campos D, Lotufo CM et al: Morphine peripheral analgesia depends on activation of the PI3Kgamma/AKT/nNOS/NO/KATP signaling pathway. Proc Natl Acad Sci USA, 2010; 107: 4442–47

45. Heinisch S, Palma J, Kirby LG: Interactions between chemokine and mu-opioid receptors: Anatomical findings and electrophysiological studies in the rat periaqueductal grey. Brain Behav Immun, 2011; 25: 360–72

46. Szabo I, Chen XH, Xin L et al: Heterologous desensitization of opioid receptors by chemokines inhibits chemotaxis and enhances the perception of pain. Proc Natl Acad Sci USA, 2002; 99: 10276–81